Combined Electromagnetic and Heat-Conduction Analysis of Rapid Rewarminging of Cryopreserved Tissues

Cai-Cheng Lu, *Senior Member, IEEE,* Huai-Zhi Li, and Dayong Gao

***Abstract*—In this paper, a combined solution of an electromagnetic (EM)-wave equation and head transfer equation is presented to analyze the microwave rewarming process of cryopreserved tissues. The solution process starts with an initial temperature of the tissue. The EM-field distribution inside the tissue is determined first by solving hybrid surface-volume integral equations. This solution provides a thermal source term for the heat-transfer equation. A finite-difference scheme is then applied to solve the heat-transfer equation, which determines the temperature distribution inside the tissue for the next time step. Since the tissue's electrical characteristics (ε and σ) are functions of temperature, their values are then updated based on the new temperature distribution. The iteration continues until a termination condition is satisfied. This combined iterative solution of wave equation and heat-transfer equation allows us to model the complex rewarming process. Numerical results are presented to demonstrate the application of the combined analysis approach.**

***Index Terms*—Cryopreservation, electromagnetic interaction, heat transfer, integral equation, rewarming.**

I. Introduction

PRACTICAL methods for cryopreservation of biological tissues would provide inestimable benefits to the field of medicine (e.g., the cell and organ transplantations). In the context of cryopreservation, vitrification typically refers to the avoidance of ice crystals with size large enough to cause cell damage [1], [2], [14]–[17]. All practical cryopreservation protocols require biological tissues to survive two perilous processes: cooling down to cryogenic storage temperature and the subsequent rewarming. In many aspects, the threats to cell viability are greater during the rewarming phase [3]. This is particularly true if the approach used during the cooling process produced a nonequilibrium phase (i.e., a vitreous solid). The prevailing view of vitrification is that numerous ice nuclei form during the cooling process, but then find themselves in an environment too viscous to permit detectable growth. These nuclei are preserved in the vitreous solid until the sample is rewarmed. During the rewarming process, these nuclei may grow at extremely rapid rates into damaging ice particles. Typically, vitrified aqueous solutions present in biological systems will begin to reorganize into crystalline forms once the temperature is raised to about -40 °C [1]. The traditional approach to minimizing this problem is to rewarm the sample as quickly as possible. This minimizes ice crystal damage by traversing the range of temperatures, where there is both a significant thermodynamic driving force toward crystallization and a significant degree of molecular diffusion. Unfortunately, avoiding formation of ice during rewarming would require heating rates ($\sim 10^6$ °C/min) that are very difficult to achieve. The chief impediment is that biological tissues have relatively low thermal conductivities and high specific heats. Moreover, care must be taken to avoid the large temperature gradient within the tissue, which may cause high thermal stress inducing tissue fracture.

The use of microwaves for rewarming offers some significant advantages over conventional methods. Since heat is generated volumetrically, the low thermal conductivity of biological materials is not so problematic. Additionally, with proper design, microwave energy can be dissipated into a material at very high rate [4]. Although these advantages have long been recognized, there has been little progress toward widespread application of microwave heating processes to avoid devitrification. Perhaps the greatest disadvantage to the use of microwaves is that heating processes require very careful design to achieve the intended outcome and avoid undesired effects (such as the formation of the hot spot in the tissue during microwave heating).

One of the reasons is due to the complicated interaction of the electromagnetic (EM) field and materials. In the heating process, the fields in an empty cavity will be distorted because of the presence of the materials. The field pattern inside the material depends on a number of factors such as the shape, size of the material, the operating frequency, and, most importantly, the constitutive parameters of the material. As a result, it is problematic to obtain the desired heating pattern or precisely control the temperature distribution. It is known that the EM field in an electrically small tissue is uniform if illuminated by a uniform external field. This means low frequency is preferred for heating a tissue of a given size. However, lower frequency microwave has a lower heating rate. Therefore, it is difficult to achieve uniform and rapid heating at the same time in a microwave cavity.

Theoretical and experimental researches are needed to better understand the microwave heating process and search for optimum design to realize the desired uniform heating. Theoretical method has the following two advantages. 1) It can provide

Manuscript received November 24, 1999; revised February 20, 2000. This work was supported in part by the Office of Naval Research under Grant N000140010605, by the Whitaker Foundation under a grant, and by the American Cancer Society under Grant RPG-00-092-01-LBC.

C.-C. Lu is with the Department of Electrical Engineering, University of Kentucky, Lexington, KY 40506 USA.

H.-Z. Li and D. Gao are with the Department of Thermal Science and Energy Engineering, University of Science and Technology of China, Hefei, Anhui, China and also with the Department of Mechanical Engineering, University of Kentucky, Lexington, KY 40506 USA.

Publisher Item Identifier S 0018-9480(00)09870-7.

detailed field and temperature pattern in the tissue. These patterns are difficulty to measure without interfering with the applied field. 2) It is a cost-effective way to simulate and compare various cases with different tissue parameters and system configurations. Extensive theoretical analysis of EM fields inside dielectric spheres have been given by several researchers [4], [5]. These results demonstrated that the EM field and, hence, the temperature inside a tissue, are very sensitive to tissue's size, shape, and electric and thermal properties. These studies were restricted to spherical samples in an open area. Though four plane waves were used in [4] to simulate the field in a rectangular cavity, it lacks the flexibility to model cavities of other shapes.

Since interaction of microwave energy with real dielectric materials is nonlinear, an authentic model of microwave heating should take this into account. Moreover, an accurate model should simulate the manner in which a dielectric material affects the $\vec{E}$-field as it is being warmed. For most materials, the dielectric properties vary with the temperature. This change can significantly distort the electric-field distribution over the course of the heating process. In either case, the electric-field distribution is altered. Since this is equivalent to change the internal heating source terms in the heat-transfer equation, it is important to include this phenomena in any model of the heating process.

Recently, Francois [6] and Ma [7] reported results using the finite-difference time-domain (FDTD) method as EM solver, and finite-difference (FD) method as heat-transfer equation solver to simulate the microwave heating process. In these simulations, the temperature pattern is calculated for a rectangular dielectric sample in a rectangular cavity. Their models have been taken into consideration of the temperature dependence for the material's electric parameters and, hence, are very close to reality. Theoretically, the FDTD method can be used to model structures of arbitrary shapes; it is difficult to implement in practice, especially when both the cavity walls and sample shapes are of curved shapes.

In this paper, we present a new method, which can handle arbitrary structure shapes, for the combined EM and heat-transfer simulation of microwave rewarming process. In this method, the EM solver is based on the numerical solution of coupled integral equations. It models the cavity wall by a set of small triangles and represents the dielectric tissue by a set of small tetrahedrons. This model provides the flexibility to simulate realistic cavities and tissue shapes. Since our ultimate interest is in the thermal effect, accurate knowledge of the temperature distribution is crucial to achieve basic understanding, the control, and optimization of the heating processes. This requires the solution of the energy equations within the processed materials. In this paper, the control volume method developed by Patankar [8] is used to model heat transfer in biological samples. The inhomogeneity nature of the tissue's electric and physical properties has been considered in the combined analysis.

The organization of this paper is as follows. Section II presents the general formulation of the problem. Then in Sections II and III, numerical schemes are discussed for the EM solver and the heat-transfer solver, respectively. Numerical simulations are shown in Section IV. Section V presents a summary of this paper and point out the directions of future work. The time factor used in representing the EM fields is $\exp(-i\omega t)$ and is suppressed.

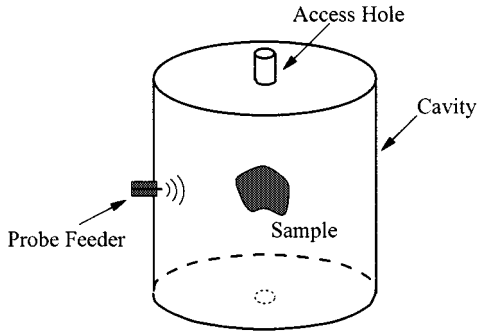

Fig. 1. Geometry sketch of a microwave rewarming cavity. The cylindrical cavity is fed by a probe near the sidewall. A tissue sample is put at the center of the cavity. Two small holes are cut at the upper and bottom end covers of the cavity for temperature monitoring. For safety reasons, pipes of small diameters are attached to the holes to attenuate the fields leaked from the opening.

II. General Formulation of the Problem

The configuration of the rewarming system is shown in Fig. 1. It consists of a microwave cavity and dielectric material (tissue sample). There are two small holes on the top and bottom cover of the cavity that are cut for temperature measurement access. The microwave power is fed in through a probe. Due to the presence of the tissue sample, the field distribution in the cavity will be different from that when the cavity is empty. In the microwave rewarming process, one is interested in the field distribution inside the sample. It is known that when the size of the tissue is much smaller than a wavelength (in material), the field in the sample will be uniform. If the size is comparable to or larger than a wavelength, then the interior field pattern is generally not uniform. In this case, it is important to know the exact field distribution. This information is important to determine whether a thermal run away will occur. The thermal run away is a phenomena in microwave heating in which the temperature in certain portion of the sample increases much faster than the rest portion, causing sever damage to the tissue or preventing the sample from being further heated to the desired temperature distribution.

For given dielectric parameters of the tissue (ε, σ, and μ), the electric-field distribution in the tissue can be determined by solving a coupled surface and volume integral equations [9], one formulated on the surface of the cavity, and one formulated in the tissue volume region

$$\left[i\omega\mu\int_S \vec{\vec{G}}(\vec{r},\vec{r}')\cdot\vec{J}_S(\vec{r}')dS' + i\omega\mu\int_V \vec{\vec{G}}(\vec{r},\vec{r}')\cdot\vec{J}_V(\vec{r}')dS'\right]_{\tan} = -\vec{E}^{\text{inc}}_{\tan}, \qquad \vec{r}\in S \tag{1}$$

$$\vec{E} = \vec{E}^{\text{inc}} + i\omega\mu\int_S \vec{\vec{G}}(\vec{r},\vec{r}')\cdot\vec{J}_S(\vec{r}')\,dS' + i\omega\mu\int_V \vec{\vec{G}}(\vec{r},\vec{r}')\cdot\vec{J}_V(\vec{r}')\,dS', \qquad \vec{r}\in V. \tag{2}$$

where $\vec{\vec{G}}$ is the free-space dyadic Green's function, $\vec{J}_S$ (A/m) and $\vec{J}_V$ (A/m^2) are the surface current and volume current, re-

spectively, and $\vec{E}^{\text{inc}}$ (V/m) is the excitation field, which is generated by the probe in the absence of the cavity and sample. The subscript "tan" stands for taking the tangent component of the corresponding quantities. Note that since the total electric field $\vec{E}$ is related to the volume current by $\vec{J}_V = i\omega(\varepsilon - \varepsilon_b)\vec{E}$, there are actually two unknown functions, i.e., $\vec{J}_S$and $\vec{J}_V$, in the two integral equations (1) and (2).

With known electric-field distribution $\vec{E}$ for every grid point in the tissue, the absorbed power density by the tissue is determined by

$$q(\vec{r}) = \frac{1}{2}\sigma\left|\vec{E}(\vec{r})\right|^2 \quad \text{W/m}^3 \tag{3}$$

where σ is the conductivity of the tissue and it is generally a function of position. The absorbed power per unit volume is then used as the thermal source term in the heat-transfer equation. Since, in this paper, the rewarming range concerned is between -196 °C and -15 °C, the phase change is assumed negligible. Without the phase change, the heat-transfer equation has the following form:

$$\rho C\frac{\partial T}{\partial t} = q(\vec{r}) + \frac{\partial}{\partial x}\left(k\frac{\partial T}{\partial x}\right) + \frac{\partial}{\partial y}\left(k\frac{\partial T}{\partial y}\right) + \frac{\partial}{\partial z}\left(k\frac{\partial T}{\partial z}\right). \tag{4}$$

where ρC (J/m^{3}K) is the volumetric heat-transfer capacity, k (W/mK) is the thermal conductivity, T (K) is the temperature, and t (s) is the time. By solving (4), one obtains the temperature distribution for the tissue as a function of time. Based on the temperature distribution, the tissue's constitutive parameters ε (F/m) and σ (S/m) are then updated using a model that is obtained experimentally. The new values of ε and σ are then fed into the EM solver again to determine the electric-field distribution. This process is repeated until a desired temperature distribution is achieved.

It can be seen from the above process that, for an initial uniform temperature distribution and uniform dielectric parameters of the tissue, the final temperature may be nonuniform due to nonuniform electric-field distribution. When the nonuniformity of the temperature distribution exceeds a certain threshold, the heating process is considered as unacceptable. Hence, maintaining the nonuniformity within a tolerance in the tissue is an important issue in microwave rewarming.

III. Solution of Wave Equations and Heat-Transfer Equations

A. Solution for EM Fields

The coupled integral equations (1) and (2) are solved simultaneously using the method of moments (MoM) [10], [14]. To this end, the surface is modeled by a set of triangles, and the sample is represented by a set of tetrahedrons. This discretization is flexible to model cavities and samples of arbitrary shapes. This is important since, in practice, the tissues to be rewarmed take many different shapes. An example of the meshed geometry is shown in Fig. 2, in which the cavity is a cylindrical resonator, and the sample is a solid sphere.

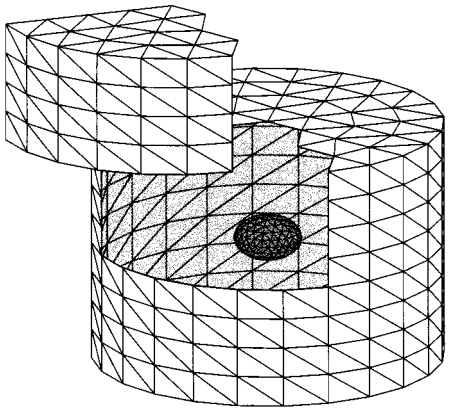

Fig. 2. Mesh of a rewarming configuration. The cavity wall is modeled by a set of small triangular patches, and the sample is modeled by a set of tetrahedrons. A portion of the cavity wall is cut and shifted for the purpose of visualization. The size of the triangular cell is about one-tenth of a free-space wavelength, and the size of the tetrahedron is close to one-tenth of dielectric wavelength.

The unknown current distributions are approximately expanded by two sets of vector basis functions: one for the surface current [11] and one for the volume current [9], [12]

$$\vec{J}_S(\vec{r}) \approx \sum_{n=1}^{N_S} a_n^S \vec{f}_n^S(\vec{r}) \tag{5}$$

$$\vec{J}_V(\vec{r}) \approx \sum_{n=1}^{N_V} a_n^V \vec{f}_n^V(\vec{r}) \tag{6}$$

where a_n^S and a_n^V are the expansion coefficients, $\vec{f}_n^S$ is the basis function for the surface current, $\vec{f}_n^V$ is the basis function for the volume current, and N_S and N_V are the number of basis functions on the surface and volume regions, respectively. If we consider a triangle or a tetrahedron as a general mesh cell, then each basis function is defined over two adjacent cells that share a same entity (the edge for triangle and the face for tetrahedron). When the cell size is small enough, (5) and (6) will give very accurate representation of the currents. When (5) and (6) are substituted into (1) and (2), and the resultant equations are tested by Galerkin's testing procedure, we will obtain a set of $N_S + N_V$ linear equations, which relate the expansion coefficients and excitation field. Thus, the unknown expansion coefficients in (5) and (6) can be solved for by a matrix inversion scheme or by an iterative solver. Finally, the electric-field distribution inside the cavity (including the sample region) can be obtained by integrate the currents given by (5) and (6).

B. Solution for Temperature Distribution

The energy absorption by a lossy dielectric material (in our case, the liquid and possibly the container) in a microwave field is described by (4). Considering the nature of microwave heating process, the magnitude of heating time is second. Furthermore, microwave heating intensity is much stronger than that of natural convection. Thus, natural convection in a microwave resonant cavity is ignored, and an adiabatic boundary condition is adopted. Equation (4) is numerically solved by the explicit controlled volume method. In this method, the material is divided into small rectangular cubes, and the current temperature at the

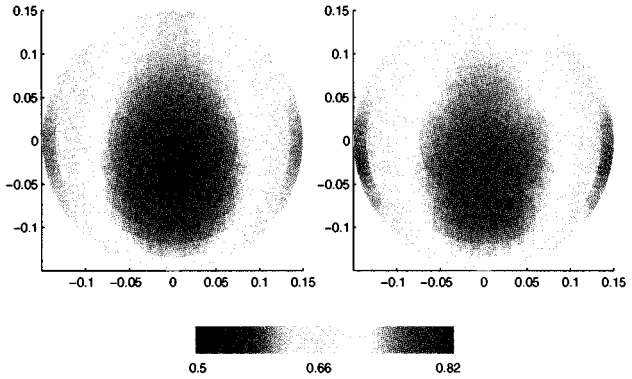

Fig. 3. Absolute value of the field intensity on the $x = 0$ cutting plane inside a dielectric sphere when the sphere is in free space and is illuminated by a plane wave. The parameters for this example are: sphere radius $= 0.15$ m, frequency $= 300$ MHz, dielectric permittivity is $3.3+1.0i$. Incident plane wave amplitude is 1 V/m and the incident direction is $\theta^i = 0°$. Both analytic solution (left-hand side) and numerical solution (right-hand side) are shown.

center of each cube is updated using the previous temperature at the current cube as well as the previous temperatures at neighboring cubes based on the following equation [8]:

$$a_p T_p = a_E T_E^0 + a_W T_W^0 + a_N T_N^0 + a_S T_S^0 + a_T T_T^0 + a_B T_B^0 + a_P T_P^0 + b. \quad (7)$$

In the above, the subscript "p" is an index of grid point, T^0 is the temperature of the previous time step, and T_p is the temperature of the current time step at grid point "p." Other symbols are described in detail in [8]. The last term in (7) is the thermal source term that is calculated using the electric-field amplitude as follows:

$$q = \frac{1}{2}\sigma_p \left|\vec{E}_p\right|^2 (\Delta x \Delta y \Delta z). \quad (8)$$

Note that q is a functions of positions. Equation (7) is solved iteratively for the temperature distribution across the sample grid points and over discrete time instances. During the iteration process, the material permittivities at all the grid points are monitored. If the maximum change of a permittivity at a grid point is greater than a pre-specified amount, the permittivities at all the points are then updated, and the EM-field solution is repeated for the new permittivity distribution. The temperature characteristic of the materials is based on a measurement model.

IV. Simulation Results

In the following, we present numerical results for the EM field as well as temperature calculations for a number of configurations. The EM solution is first compared with the analytic solution for uniform dielectric sphere, and then the code is applied to calculate the electric-field distribution in tissue samples of spherical shape and rectangular cubic shape. The tissues used in the examples are similar to the perfused rabbit kidney given in [13]. Figs. 3–6 show the simulation results. In Fig. 3, the absolute field-intensity values are plotted and, in Figs. 4–6, the field intensity relative to the minimum field intensity is plotted. The thermal parameters used in this paper's simulation are $\rho C = 2.01$ (MJ/m^{3}K), $k = 5.69 \times 10^{-3}$ (W/mK).

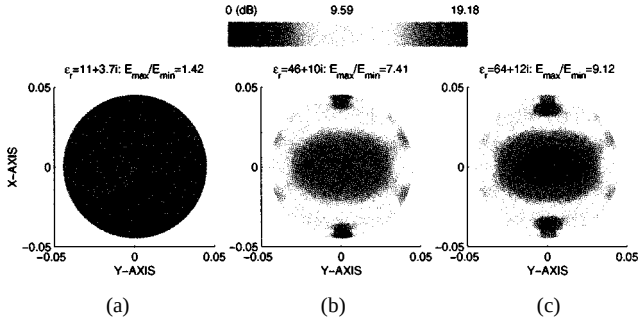

(a) (b) (c)

Fig. 4. Relative field-intensity comparison for three dielectric spheres of uniform permittivity. (a) $\varepsilon_r = 11+3.7i$. (b) $\varepsilon_r = 46+10i$. (c) $\varepsilon_r = 64+12i$. In each plot, 0 dB stands for $|E_{\min}|$.

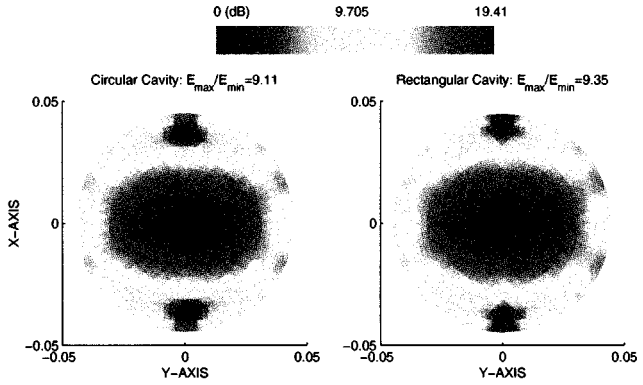

(a) (b)

Fig. 5. Field patterns of a dielectric sample when it is put: (a) in a circular cylindrical cavity and (b) in a rectangular cavity.

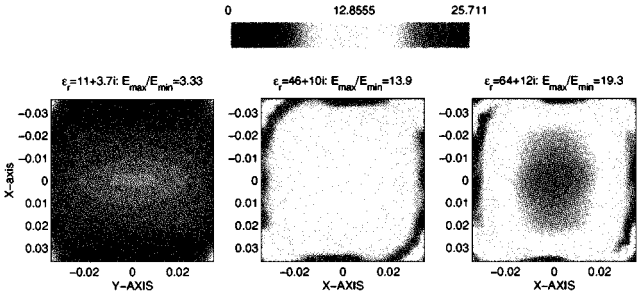

(a) (b) (c)

Fig. 6. Field pattern of a cubic sample at three temperatures. This should be compared with the patterns shown in Fig. 4 for a spherical sample of the same volume.

A. Comparison with Analytic Solution

First, we calculate the interior field distribution for a homogeneous sphere in free space that is illuminated by a plane wave of unit amplitude (1 V/m). For this configuration, an analytical solution exists. This example is to show that the developed algorithms have the required solution accuracy. The calculated electric-field-intensity distribution (in volts per meter) on the $x = 0$ cutting plane is shown in Fig. 3. As a comparison, the analytical solution is shown in Fig. 3. In this example, the field nonuniformity, defined as the ratio of the maximum and minimum field intensities, is 1.39 (the result from the analytic solution is 1.42).

B. Dielectric Sphere in Cavities

Next, we will calculate the field distribution in a dielectric sphere when it is put inside a circular cavity. This example is to show the effect of the dielectric constant on the field pattern. The radius and height of the cavity are 0.26 and 0.55 m, respectively, and it supports a TE_{111} mode at 434 MHz. It is excited by a short coaxial probe inserted into the cavity at the center of the sidewall. For the simulation examples given in this paper, the probe is considered as a short dipole, and the accessing holes on the cavity covers are sealed.

Hence, the primary field is that of a short dipole in the absence of the cavity and the sample, i.e., the field on the right-hand side of (1) and (2). The field in the cavity and the sample is calculated by solving the coupled surface-volume integral equations. The sample is a dielectric sphere and is located at the center of the cavity. The sample has the dielectric properties as the perfused rabbit kidney tissue given in [13, Table I]. At a frequency of 434 MHz and temperatures of -30 °C, -12 °C, and 0 °C, the tissue permittivities are $11.0+i3.7$, $46.0+i10.0$, and $64.0+i12.0$, respectively. The radius of the dielectric sphere is 50 mm. In the discretization, the sphere is represented by 480 small tetrahedrons, and the cavity wall is represented by 526 small triangles. In order to compare the electric-field nonuniformity for the three cases, the relative field intensity $\tilde{E} = |\vec{E}|/|\vec{E}|_{\min}$ is plotted. It is clear that the maximum value of $\tilde{E}$ indicates the nonuniformity of the fields across the sample's interior points. Uniform heating means $\tilde{E} = 1$ for all points in the sample. In the following figures, the displayed patterns are the log value of the relative electric-field intensity (hence, the minimum electric-field intensity corresponds to 0 dB).

Fig. 4 shows the relative electric-field intensity for the three temperatures when the sample is put in the circular cavity (again, absolute field values from the three cases are quite different. However, we are interested in the uniformity of the fields; hence, the relative intensity is plotted. For each case, the minimum field intensity is used as reference, or 0 dB).

It can be seen from Fig. 4 that with the increase in temperatures, the nonuniformity of the field distribution is also increased, causing nonuniform heating.

C. Circular Versus Rectangular Cavity

In order to study the effect of the cavity shapes on the field distribution, the calculation results are compared for a circular cavity (Section IV-B) and a rectangular cavity. The rectangular cavity is designed so that the TE_{101} mode resonates at 434 MHz. The dimensions are $a = 0.52$ m, $b = 0.27$ m, and $c = 0.345$ m, where a, b, and c are the dimensions in the x-, y-, and z-directions. The coordinate is chosen such that the center of the cavity is at the origin. The cavity is excited also by a short dipole located at $(0, -0.1, 0)$. Fig. 5 shows the differences in the pattern distribution when the sample is in circular and rectangular cavities. For this particular case, the difference in the field pattern is not significant.

D. Spherical Versus Cubic Samples in Circular Cavity

It is generally accepted that the field pattern uniformity is dependent on the shape of the sample. The detailed quantitative comparison can be obtained through simulation. In the next example, a spherical and cubic sample are put in a circular cylinder, one at a time. The two samples have the same volume and dielectric properties. The radius of the spherical sample is 0.05 m, and its field pattern is shown in a previous figure (Fig. 4). The side length of the cubic sample is set to 0.0806, and its field pattern is shown in Fig. 6. As is expected, the temperatures near the corners are higher than the other parts on the sample due to field singularities at those places.

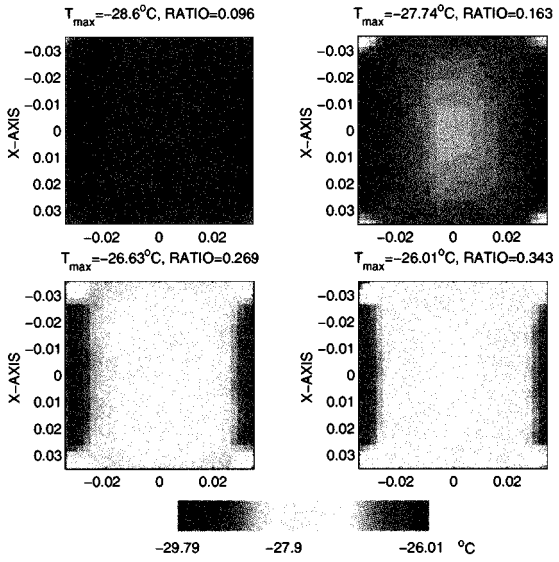

Fig. 7. Temperature pattern for a cubic sample obtained iteratively using the combined EM and heat-transfer equation solution. The pattern are taken at the $z = 0$-plane in the sample. The RATIO shown in the figure is defined as $(T_{\max} - T_{\min})/T_{\mathrm{ave}}$ for the corresponding data set.

E. Combined Solution Example

In practical rewarming, the temperature has a large variation range, say, from -60 °C to 0 °C. It can be expected that, with this range, the temperature, initially uniform, can become highly nonuniform at the end of the rewarming process. We found that this is true even within a small temperature variation range. In the last example, we demonstrate the variation of the temperature nonuniformity during a heating (or rewarming) process by considering a cubic sample in a circular cavity. The sample that resembles the perfused rabbit kidney is used for this simulation. It is a cubic with side length of 0.0806 m, and is put at the coordinate origin, which is also the center of the cavity. The initial temperature is assumed to be uniform (-30 °C across the sample), and the permittivity of the sample at this temperature is $\varepsilon_r = 11.0 + 3.7i$. The simulation starts by solving for the electric-field distribution. The heat source is then calculated based on (8). Finally, the heat-transfer equation is solved to obtain the temperature of the next step. With the new temperature, the permittivity distribution is updated (hence, the sample's permittivity becomes nonuniform). In this example, a three-point interpolation model is used to update the permittivity in the temperature range from -30 °C to -20 °C. The three measured data samples are [13] $(T, \varepsilon_r) = (-30°\mathrm{C}, 11.0 + i3.7)$, ($-25$ °C, $13.0 + i4.55$), (-20 °C, $19.0 + i7.03$). Temperature patterns taken at the $z = 0$ plane in the sample are plotted in Fig. 7. It

can be seen that the nonuniformity becomes high with the increase of temperatures. The center of the sample and the region near the corners are heated more compared to the rest of the region.

V. Summary

In this paper, an iteration algorithm is presented to obtain the EM-field distribution and the temperature pattern for arbitrary shaped samples when they are in free space and inside cavities. The iteration involves solving the EM wave equation and the heat-transfer equation alternatively. The EM solver models the cavity with triangular patches and the dielectric tissue by tetrahedrons. Hence it can be used to simulate realistic microwave rewarming and heating processes, and provides an accurate and effective tool for virtual experiments, through which we can analyze the heating pattern and the heating rate as functions of a sample's size, shape, and electric and heat-conduction properties. These simulations are essential to know what kind of cavity and what control process can lead to a desired heating pattern and rewarming history.

References

[1] G. M. Fahy, "Vitrification," in *Proceedings of NATO Advanced Study Institute on Biophysics of Organ Cryopreservation*. New York: Plenum, 1987, pp. 133–147.

[2] ——, "Vitrification of multicellular systems and whole organs," *Cryobiol.*, vol. 24, p. 581, 1987.

[3] T. Nei, "Mechanism of hemolysis of erythrocytes by freezing at near-zero temperatures—I. Microscopic observation of hemolyzing erythrocytes during the freezing and thawing process," *Cryobiol.*, vol. 4, pp. 153–156, 1967.

[4] X. Bai, D. E. Pegg, S. Evans, and J. D. J. Penfold, "Analysis of electromagnetic heating patterns inside a cryopreserved organ," *J. Biomed. Eng.*, vol. 14, pp. 459–466, Nov. 1992.

[5] J. D. J. Penfold and S. Evans, "Control of thermal runaway and uniformity of heating in the electromagnetic rewarming of a cryopreserved kidney phantom," *Cryobiol.*, vol. 30, pp. 493–508, 1993.

[6] L. Ma, D. L. Paul, N. Pothecary, C. Railton, J. Bows, L. Barratt, J. Mullin, and D. Simons, "Experimental validation of a combined electromagnetic and thermal FDTD model of a microwave heating process," *IEEE Trans. Microwave Theory Tech.*, vol. 43, pp. 2565–2571, Nov. 1995.

[7] F. Torres and B. Jecko, "Complete FDTD analysis of microwave heating processes in frequency-dependent and temperature-dependent media," *IEEE Trans. Microwave Theory Tech.*, vol. 45, pp. 108–116, Jan. 1997.

[8] S. A. Patankar, *Numerical Heat Transfer and Fluid Flow*. Seattle, WA: Hemisphere, 1980.

[9] C. C. Lu and W. C. Chew, "Electromagnetic scattering from material coated PEC objects: A hybrid volume and surface integral equation approach," in *1999 IEEE AP-S Int. Symp. Dig.*, Orlando, FL, July 1999, pp. 2562–2565.

[10] R. F. Harrington, *Field Computation by Moment Methods*. New York: Macmillan, 1968.

[11] S. M. Rao, D. R. Wilton, and A. W. Glisson, "Electromagnetic scattering by surfaces of arbitrary shape," *IEEE Trans. Antennas Propagat.*, vol. AP-30, pp. 409–418, Mar. 1982.

[12] D. H. Schaubert, D. R. Wilton, and A. W. Glisson, "A tetrahedral modeling method for electromagnetic scattering by arbitrary shaped inhomogeneous dielectric bodies," *IEEE Trans. Antennas Propagat.*, vol. AP-32, pp. 77–85, Jan. 1984.

[13] S. Evans, M. J. Rachman, and D. E. Pegg, "Design of a UHF applicator for rewarming of cryopreserved biomaterials," *IEEE Trans. Biomed. Eng.*, vol. 39, pp. 217–225, Mar. 1992.

[14] M. N. O. Sadiku, *Numerical Techniques in Electromagnetics*. Boca Raton, FL: CRC Press, 1992.

[15] D. Y. Gao, T. Jackson, and W. Zhang, "Development of a novel microwave cavity to vitrify biological tissues for use in surgical transplantation," in *Advances in Heat and Mass Transfer in Biotechnology*, S. Clegg, Ed. New York: ASME Press, 1997, vol. HTD-335/BED-37, pp. 185–190.

[16] T. H. Jackson, A. Ungan, J. K. Critser, and D. Y. Gao, "A novel means of enhancing vitrification of biomaterials by microwave irradiation during cooling," *Cryobiol.*, vol. 34, pp. 363–372, 1997.

[17] D. Y. Gao, Q. Zhang, and H. Z. Li, "Application of microwave irradiation to cryopreservation of biomaterials," in *Proc. BEMS–EMBS'99*, Atlanta, GA, p. 1287.

Cai-Cheng Lu (S'95–M'95–SM'98) received the B.S. and M.S. degrees from the Beijing University of Aeronautics and Astronautics, Beijing, China, in 1983 and 1986, respectively, and the Ph.D. degree from the University of Illinois at Urbana-Champaign, in 1995.

From 1986 to 1991, he was with the Department of Electronic Engineering, Beijing University of Aeronautics and Astronautics. From 1992 to 1997, he was with the Department of Electrical and Computer Engineering, University of Illinois at Urbana-Champaign, first as a Graduate Research Assistant and then as a Research Scientist. He has been involved with antenna design and measurement, fast algorithms for EM scattering, and inverse scattering. He also participated in the development of the fast Illinois solver code (FISC). In 1998, he joined Demaco Inc., where he was involved with asymptotic techniques for radar scattering predictions. He is currently an Assistant Professor in the Department of Electrical Engineering, University of Kentucky, Lexington. His research interests include fast algorithms for wave scattering and inverse scattering, antenna analysis and design, and EM biomedical applications.

Dr. Lu is a member of Phi Kappa Phi. He was the recipient of the 2000 Young Investigator Award presented by the Office of Naval Research.

Huai-Zhi Li is currently with the Department of Mechanical Engineering, University of Kentucky, Lexington.

Dayong Gao received the B.S. degree in mechanical engineering from the University of Science and Technology of China, Hefei, Anjui, China, in 1982, and the Ph.D. degree in mechanical engineering from Concordia University, Montreal, PQ, Canada, in 1991.

He is currently an Associate Professor of mechanical engineering and bioengineering in the Department of Mechanical Engineering, University of Kentucky, Lexington. Prior to joining the University of Kentucky, he was a Senior Scientist and Group Leader in the Cryobiology Research Institute, Indianapolis, IN. He has authored or co-authored numerous publications in cryobiology research and holds seven U.S. patents. His research has focused on fundamental and applied cryobiology and biotechnology. His research interests include fundamental cryobiology of mammalian cells (sperm, oocytes, platelets, hematopoietic stem cells) and tissues (embryos, arteries, and corneas) and the development of novel techniques and equipment for cell/tissue cryopreservation.

Dr. Gao has been a member of the Society for Cryobiology since 1987. He was elected to serve as Treasurer of the Society of Cryobiology and committee member of the K-17 Committee on Advanced Bio-Heat and Mass Transfer of the American Society of Mechanical Engineers (ASME). He has been the recipient of grants and awards from the American Cancer Society, American Heart Association, National Institutes of Health (NIH), Whitaker Foundation, Department of Defense (DoD), National Science Foundation (NSF), and industries.